JACS
JOURNAL OF THE AMERICAN CHEMICAL SOCIETY
Article
pubs.acs.org/JACS

Dynamic, Reversible Oxidative Addition of Highly Polar Bonds to a Transition Metal

Rüdiger Bertermann,[†,‡] Julian Böhnke,[†,‡] Holger Braunschweig,*[,†,‡] Rian D. Dewhurst,[†,‡] Thomas Kupfer,[†,‡] Jonas H. Muessig,[†,‡] Leanne Pentecost,[§] Krzysztof Radacki,[†,‡] Sakya S. Sen,[‡,∥] and Alfredo Vargas[§]

[†]Institute for Sustainable Chemistry & Catalysis with Boron, and [‡]Institute for Inorganic Chemistry, Julius-Maximilians-Universität Würzburg, Am Hubland, 97074 Würzburg, Germany

[§]Department of Chemistry, School of Life Sciences, University of Sussex, Brighton, Sussex BN1 9QJ, United Kingdom

[∥]Catalysis Division, CSIR - National Chemical Laboratory, Pashan, Pune 411008, India

Supporting Information

ABSTRACT: The combination of Pt^0 complexes and indium trihalides leads to compounds that form equilibria in solution between their In−X oxidative addition (OA) products (Pt^{II} indyl complexes) and their metal-only Lewis pair (MOLP) isomers ($L_nPt\rightarrow InX_3$). The position of the equilibria can be altered reversibly by changing the solvent, while the equilibria can be reversibly and irreversibly driven toward the MOLP products by addition of further donor ligands. The results mark the first observation of an equilibrium between MOLP and OA isomers, as well as the most polar bond ever observed to undergo reversible oxidative addition to a metal complex. In addition, we present the first structural characterization of MOLP and oxidative addition isomers of the same compound. The relative energies of the MOLP and OA isomers were calculated by DFT methods, and the possibility of solvent-mediated isomerization is discussed.

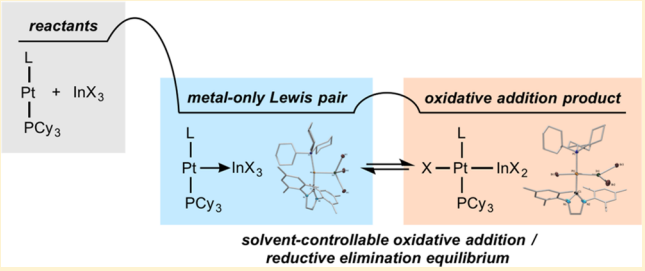

INTRODUCTION

The oxidative addition of an element−element bond to a transition metal is one of the most important concepts in organometallic chemistry and its related applications in organic, catalytic, and industrial chemistry.[1] Although oxidative addition is often a reversible process, the observation of well-defined oxidative addition (OA)/reductive elimination (RE) equilibria is quite rare. Dihydrogen is the most exemplary of these cases, where the metal dihydride oxidative addition product [$L_nM(H)_2$] and the corresponding side-on-bound dihydrogen σ complex [$L_nM(\sigma\text{-}H_2)$] are often found to be in equilibrium (Figure 1, middle).[2] A similarly flat energetic profile links the OA and RE products of hydrosilane[3] and hydroborane[4] addition to metal complexes. In the presence of mixtures of similar alkanes, certain metal complexes have also been found to generate mixtures of competing C−H oxidative addition products, implying reversible oxidative addition.[5]

To our knowledge, the most polar bond known to be involved in an observable OA/RE equilibrium is Sn−Cl, in one report by Puddephatt in 1995,[6] where the (Pauling) electronegativity difference between the two atoms (Δ_{EN}) is 1.20. Other bonds that have led to observed reversibility or OA/RE equilibrium mixtures are C−X (X = Cl, Br, I; Δ_{EN} 0.11−0.61),[7] C−S (Δ_{EN} 0.03),[8] B−B (Δ_{EN} 0),[9] and Se−Se (Δ_{EN} 0).[10] In 2012, we uncovered a reversible insertion of Pt^0 into an Au−Cl bond (Δ_{EN} 0.62);[11] however, the classification of this reaction as an oxidative addition is a matter of debate. The same year we also reported an "interrupted" B−C bond (Δ_{EN} 0.51) oxidative addition product derived from a borirene, which was shown from structural and spectroscopic analysis to exist in a state somewhere between the OA and σ-BC extremes.[12] Nevertheless, it is clear that observable OA/RE equilibria are very rare with highly polar bonds, perhaps due to a synergic thermodynamic preference for M−E and M−X bonds over the formation of an E−X bond and a low-valent metal fragment.

In our efforts to expand the known range of unsupported metal-only Lewis pairs (MOLPs),[13,14] complexes with metal-to-metal dative bonds ($L_nM\rightarrow M'L'_n$), we turned to reactions between indium trihalides and zerovalent platinum complexes. To our surprise, a number of these reactions produced well-defined equilibrium mixtures between the products of oxidative addition of the highly polar In−X bonds (Δ_{EN} 0.88−1.38) and their MOLP counterparts (RE products). The position of the equilibria could be altered reversibly by changing the solvent, and both reversibly and irreversibly by the addition of further donor ligands. In one case, both the OA and the MOLP isomers of the same molecule could be structurally characterized. These results identify MOLP complexes as alternative "pre-OA states" to the more well-known σ complexes,[2−5,15] which are capable of

Received: October 10, 2016
Published: November 21, 2016

DOI: 10.1021/jacs.6b10609
J. Am. Chem. Soc. 2016, 138, 16140−16147

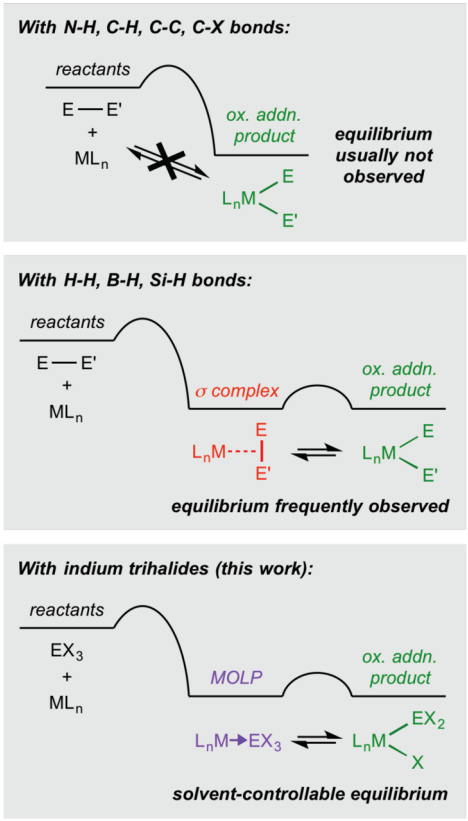

Figure 1. Illustration of how σ-complexes and MOLPs act as viable pre-OA states of comparable energy to their respective OA products, leading in some cases to observable equilibria.

establishing OE/RE equilibria by virtue of their energies being similar to those of the OA products (Figure 1).

RESULTS AND DISCUSSION

Reaction of In^{III} Trihalides with Pt^0 Complexes. Our previous investigations into the reactivity of Pt^0 complexes with group 13 trihalides began in earnest with the synthesis of the MOLP [(Cy$_3$P)$_2$Pt→AlCl$_3$] in 2007,[14a] which stood in contrast to the well-known oxidative additions of boron trihalides (even BF$_3$) to low-valent transition metal complexes.[16] In 2008 we reported that [Pt(PCy$_3$)$_2$] undergoes oxidative addition of Ga–X bonds with GaBr$_3$ and GaI$_3$, but instead forms a MOLP with GaCl$_3$. After these results, we turned to indium trihalides to complete the group 13 trihalide quartet. As Pt^0 precursors we employed [Pt(PCy$_3$)$_2$] as well as its bulkier NHC variant [Pt(IMes)(PCy$_3$)] (IMes = 1,3-bis(2,4,6-trimethylphenyl)-imidazol-2-ylidene), to probe the effects of sterics on MOLP formation, similar to our recent study with Fe^0→GaX$_3$ MOLPs.[14j]

Thereby, Et$_2$O solutions of [PtL(PCy$_3$)] (L = IMes, PCy$_3$) and indium halides InX$_3$ (X = Cl, Br, I) were mixed, leading in every case to spontaneous precipitation of either colorless or yellow/orange solids **1**–**6** (colorless implies a near-exclusive OA product, while yellow/orange implies at least some proportion of MOLP product; Figure 2). Because of extreme insolubility in Et$_2$O, in only two of these reactions ([PtL(PCy$_3$)] + InI$_3$) was a ^{31}P NMR signal observed from the mother liquor after separation of the solids; in both cases, these signals were attributable to the OA product, with ^{31}P chemical shifts near Δ 20–28 (**3b** and **6b**). Solid-state ^{31}P VACP/MAS NMR was performed on solids **1** and

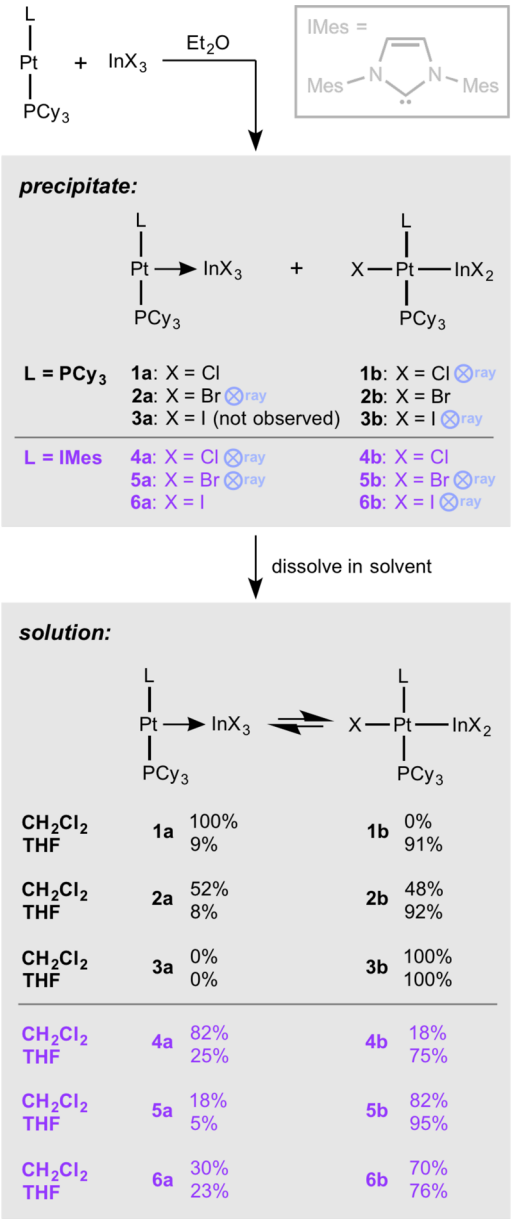

Figure 2. Reaction of Pt^0 complexes with indium trihalides, showing the resulting mixtures and solvent-dependent equilibria. IMes = 1,3-bis(2,4,6-trimethylphenyl)imidazol-2-ylidene.

2, showing the former to be almost exclusively the OA product (ratio **1a**:**1b** 2:98), and the latter to be a nearly equimolar mixture (**2a**:**2b** 52:48). While the composition of the remaining four solids were determined by solid-state NMR, all six solids were dissolved in both CH$_2$Cl$_2$ and THF, and their ^{31}P NMR spectra were measured (Table 1).

To our surprise, in a number of cases, both the OA and the MOLP products were found to coexist in solution, indicating the presence of an OA/RE equilibrium (Figure 2). On the basis of previous work,[14a] the lower-field ^{31}P NMR signals (Δ 28–49) with larger ^{31}P–^{195}Pt coupling constants (2500–2700 Hz) could be assigned to MOLP complexes (**1a**–**6a**, except **3a**), and the higher-field signals (Δ 17–33) with smaller coupling constants (1950–2050 Hz) to the OA products (**1b**–**6b**). It should be noted that in some cases the ^{31}P–^{195}Pt coupling constants could not be observed, presumably due to the quadrupolar nature of the two natural isotopes of indium (^{113}In and ^{115}In, both spin 9/

DOI: 10.1021/jacs.6b10609
J. Am. Chem. Soc. 2016, 138, 16140–16147

Table 1. NMR Shifts, Coupling Constants, Molar Ratios of a to b Isomers in Different Solvents, and Pt−In Bond Lengths for Complexes 1−6

	a Δ_P (J_{PtP})[a]	b Δ_P (J_{PtP})[a]	ratio **a**:**b**	d_{PtIn}[b]	d_{rel}
1 (solid)	48.4 (n.a.)	27.7 (n.a.)	2:98	**1b**: 2.5469(8)	0.916
1 (dcm)	48.2 (2575)	n.d. (n.d.)	100:0		
1 (thf)	49.1 (n.d.)	25.6 (2021)	9:91		
2 (solid)	47.7 (n.a.)	24.5 (n.a.)	52:48	**2a**: 2.562(3)	0.920
2 (dcm)	45.9 (2640)	32.5 (n.d.)	54:46		
2 (thf)	46.1 (n.d)	26.7 (1988)	8:92		
3 (dcm)	n.d.	27.8 (1954)	0:100	**3b**: 2.5217(6)	0.907
3 (thf)	n.d.	27.9 (1954)	0:100		
4 (dcm)	36.5 (2610)	24.6 (n.d.)	82:18	**4a**: 2.5536(8)	0.919
4 (thf)	36.8 (n.d.)	17.6 (n.d.)	25:75		
5 (dcm)	34.5 (2695)	22.7 (2016)	18:82	**5a**: 2.5468(4)	0.916
5 (thf)	36.1 (n.d.)	22.0 (n.d.)	5:95	**5b**: 2.5210(8)	0.907
6 (dcm)	27.8 (n.d.)	19.1 (2047)	30:70	**6b**: 2.5441(5)	0.915
6 (thf)	28.1 (n.d.)	19.8 (n.d.)	24:76		

[a]Δ in ppm, *J* in Hz. [b]Bond lengths in Å, n.d. not detected, n.a. not applicable.

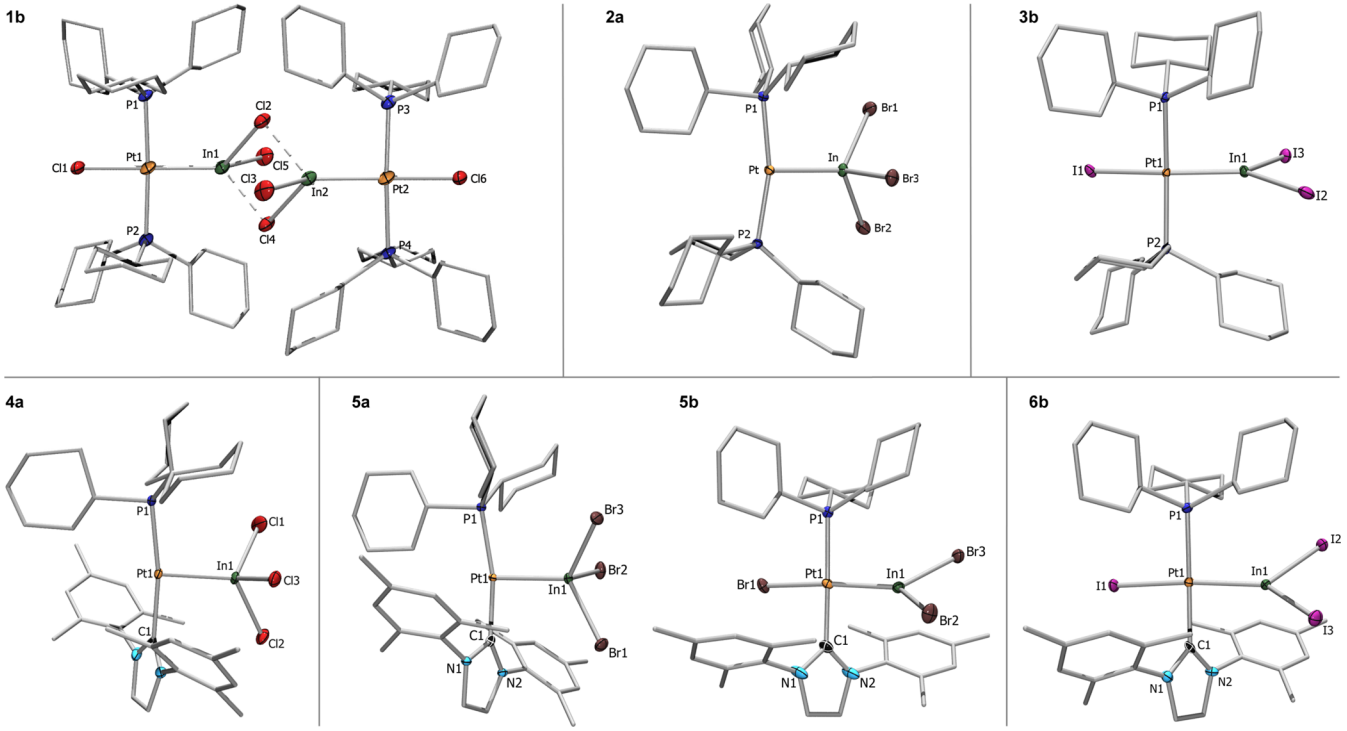

Figure 3. Crystallographically derived structures of oxidative addition products **1b**, **3b**, **5b**, and **6b**, and MOLPs **2a**, **4a**, and **5a**. Ellipsoids shown at the 50% probability level. Some ellipsoids and all hydrogen atoms and solvent molecules (one CH_2Cl_2 each for **1b**, **5a**, and **5b**) have been removed for clarity. Selected bond lengths (Å) for **1b**: Pt−In 2.5469(4), Pt−P 2.3426(8). For **2a**: Pt−In 2.562(3), Pt−P 2.282(3). For **3b**: Pt−In 2.5197(6), Pt−P 2.3348(9). For **4a**: Pt−In 2.5536(8), Pt−P 2.2838(1), Pt−C 2.016(2). For **5a**: Pt−In 2.5468(4), Pt−P 2.2818(8), Pt−C 2.011(2). For **5b**: Pt−In 2.5210(8), Pt−P 2.309(2), Pt−C 2.021(1). For **6b**: Pt−In 2.5441(5), Pt−P 2.309(2), Pt−C 2.021(1).

2) and due to the extreme broadening of the ^{195}Pt satellites caused by strong chemical shift anisotropy relaxation. The different solvents in some cases led to dramatically different proportions of the two isomers, in particular in the case of solid **1**, which gave exclusively **1a** in CH_2Cl_2 but a 9:91 mixture of **1a** to **1b** in THF. In all cases, THF favored the OA product more than did CH_2Cl_2, presumably due to interaction of the Lewis basic solvent with the nominally Lewis acidic tricoordinate indium centers of the OA products (this possibility is discussed in the DFT Calculations). In accord with our previous results with gallium trihalides, the general trend observed is that MOLPs are favored with Cl, while OA products predominate with Br and I. When considering the differences between the mono- and diphosphine complexes, neither appeared to consistently and clearly favor any particular isomer.

A variable-temperature $^{31}P\{^1H\}$ NMR experiment was undertaken with **1a**/**b** in THF, which shows nearly exclusively **1b** at 20 °C (**1a**:**1b** 11:89, K_{eq} = 8.09). Cooling the sample resulted in effectively complete disappearance of the signal for **1a** at −20 °C, while heating the sample resulted in increasing amounts of **1a** up to 40 °C, at which point **1a** and **1b** were present in a ratio 21:79. From a van't Hoff plot of ln(K) versus the inverse of the temperature, the enthalpy of the isomerization from **1a** to **1b** was calculated to be −8.10 kcal mol^{-1}, which is in the same

DOI: 10.1021/jacs.6b10609
J. Am. Chem. Soc. 2016, 138, 16140−16147

order of magnitude as that calculated by DFT methods (with THF solvent considered and one molecule of THF bound to the In atom of **1b**: −1.104; vide infra).

Single crystals of the complexes suitable for X-ray crystallography were grown by diffusion of hexane into dichloromethane solutions (**1b**, **2a**, **5a**,**b**, **6b**), or recrystallization from either Et_2O (**3b**) or toluene (**4a**). In the case of complex **5**, both colorless and orange crystals were identified in the crystal sample. One crystal of each color was measured to provide the molecular structures of isomers **5a** (orange) and **5b** (colorless). The crystallographically derived molecular structures of the complexes (Figure 3) demonstrate that the crystallized isomer is not always that which predominates in solution. It should also be noted that exclusively **1b** crystallized in a dimeric form, in which one indium-bound chloride of each complex bridges two indium centers. This phenomenon causes the Pt−In distance of **1b** (2.5469(8) Å) to be noticeably longer than those of the monomeric **3b** (2.5217(6) Å). As expected, within each set of Pt fragments, the Pt−In bond is shorter in the OA product than in the MOLP product.

Notably, the structural characterization of both **5a** and **5b** allows, for the first time, a direct comparison of the structure of a MOLP with its OA isomer. The Pt−In distance of MOLP **5a** is ca. 1% longer than that of the OA product **5b**, while the Pt−P distance of **5a** is ca. 1% shorter than that of **5b**. The Pt−C distances are effectively identical between the two isomers. These metrics argue for a very modest change in the Pt−In bonding situation upon oxidative addition, and perhaps a significant role of the covalently bound platinum−indate zwitterionic form (i.e., $Pt^{+}-In^{-}$).

As a useful measure of the relative bond distance between atoms in different metal complexes, in 2012 we introduced the metric d_{rel},[13] which is the ratio of the bond distance of interest to the sum of the experimentally derived covalent radii of the atoms ($\sum^{covrad}$(PtIn) = 2.78 Å).[17] The measured MOLPs **2a**, **4a**, and **5a** all show d_{rel} values of 0.92, only slightly lower than those of previously measured MOLPs containing Pt bound to group 13 halides (0.92−0.93). All of these values, however, are significantly lower than the average d_{rel} values of neutral MOLP complexes, as surveyed in our 2012 review article.[13]

Intermetal Lewis-Acid-Exchange Experiment. In a number of our previous reports of MOLP complexes,[14] we employed intermetal Lewis-acid-exchange reactions to directly compare the Lewis basicity of pairs of metal complexes. By adding basic metal complexes to particular MOLPs, we found that the Lewis acid fragment could be sequentially transferred from metal to metal, allowing us to determine hierarchies of basicity between TM complexes. On the basis of these results, we were interested in determining the effect of a notably stronger metal base on an existing MOLP/OA equilibrium. Thereby, when one equivalent of the stronger base [Pt(IMes)(PCy_3)] was added to an equilibrium mixture of **2a**/**b** in *o*-$C_6H_4F_2$, the resulting ^{31}P NMR spectrum showed signals for both **5a** and **5b** in a 18:82 ratio, as well as [Pt(PCy_3)$_2$] (Figure 4). This suggests that the Lewis acid is completely transferred to the superior base, the resulting MOLP then establishes an equilibrium with its OA product, and that the [Pt(PCy_3)$_2$] does not interfere with the process.

Reactivity of the MOLP/OA Equilibria. Given the existence of clear equilibria of the MOLP and OA products, we envisaged reactions with further Lewis basic ligands as a way to force the complexes to the MOLP side of the equilibrium. *o*-Difluorobenzene solutions of **1a**/**b**, **2a**/**b**, and **3b** were thus

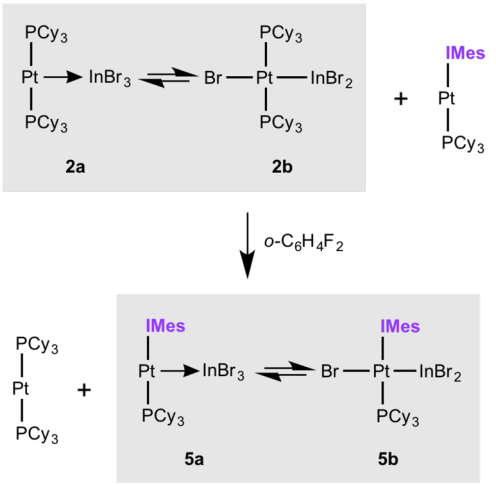

Figure 4. Intermetal Lewis-acid-exchange reaction between the equilibrium mixture **2a**/**b** and the superior metal base [Pt(IMes)(PCy_3)].

treated with solutions of isocyanide :CN*t*Bu in a greater than 4-fold excess, leading to compounds **7**−**9**, respectively (Figure 5).

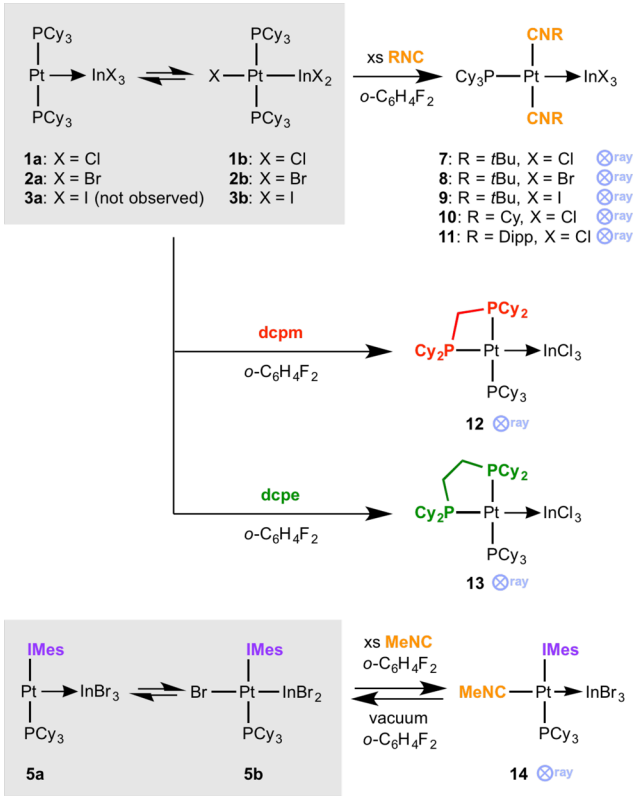

Figure 5. Reactions of Pt−In equilibria with Lewis donors: dcpm = bis(dicyclohexylphosphino)methane, dcpe = 1,2-bis(dicyclohexylphosphino)ethane (dcpe), Dipp = 2,6-diisopropylphenyl, IMes = 1,3-bis(2,4,6-trimethylphenyl)imidazol-2-ylidene.

Similarly, **1a**/**b** was treated with :CNCy and :CNDipp (Dipp = 2,6-diisopropylphenyl), providing compounds **10** and **11**. Of the solids of compounds **7**−**11**, only **9** was found to be colored (yellow). All of the compounds **7**−**11** were obtained in yields greater than 70%. The ^{31}P NMR spectra of **7**−**11** showed singlet signals in the range δ 31.8−43.8, with coupling constants in the

DOI: 10.1021/jacs.6b10609
J. Am. Chem. Soc. 2016, 138, 16140−16147

narrow range 1961−2057 Hz (Table 2). The ^{31}P NMR signals of the complexes clearly show an upfield shift as the halide becomes heavier, presumably due to the reduced σ-acidity of the heavier halides. While these data were insufficient for determining the constitution of the complexes, integration of the ^{1}H NMR data indicated the inclusion of two isonitriles per phosphine in each molecule. Unfortunately, in no case was the isonitrile carbon nucleus observed in the ^{13}C NMR spectra.

Table 2. NMR Shifts, Coupling Constants, and Pt−In Bond Lengths for the Complexes 7−14

	δ_P (mult.)[a]	J_{PtP}[b]	J_{PP}[b]	d_{PtIn}[c]	d_{rel}[d]
7	38.1 (s)	2030	n.a.	2.6205(8)	0.943
8	36.8 (s)	1983	n.a.	2.615(2)	0.941
9	31.8 (s)	1961	n.a.	2.630(1)	0.946
10	39.7 (s)	2057	n.a.	2.6059(6)	0.937
11	43.8 (s)	2032	n.a.	2.6311(6)	0.946
12	39.0 (dd)	n.d.	300, 18	2.6282(6)	0.945
	−21.7 (dd)	n.d.	300, 49		
	−26.7 (br s)	n.d.	n.d.		
13	68.4 (br s)	n.d.	n.d.	2.650(2)	0.953
	64.5 (dd)	n.d.	290, 9		
	32.4 (dd)	n.d.	290, 16		
14	20.6 (s)	n.d.	n.a.	2.661(1)	0.957

[a] δ in ppm. [b] J in Hz. [c] Bond lengths in Å, n.d. not detected, n.a. not applicable. [d] d_{rel} = metal−metal distance/$\sum$(experimental covalent radii of metals[17]).

Single crystals of **7**−**11** suitable for X-ray crystallography were grown by diffusing hexane into their *o*-difluorobenzene solutions. The crystallographically derived structures of **7**−**11** (Figure 6) confirm their connectivity as MOLPs with square-planar, four-coordinate Pt centers. Of the possible isomers, the complexes all display the least sterically hindered geometry, that is, that with mutually-*trans* isonitrile groups. It should also be noted that in complex **10**, the two cyclohexyl groups are of opposite conformation (one equatorial, one axial). In contrast to the ^{31}P NMR data, the nature of the halide appears to have little bearing on the Pt−In distance in the complexes. The complex with the shortest Pt−In distance (**8**: 2.615(2) Å) is that with the least sterically bulky isonitrile, :CNCy, which bears a tertiary carbon atom attached to N rather than the quaternary carbon of :CN*t*Bu and the bulky alkylated aryl group of :CNDipp.

Given the success of the addition of isonitriles to the equilibrium mixtures of **1**−**3**, MOLP/OA mixture **1a**/**b** was also treated with the chelating diphosphines bis(dicyclohexylphosphino)methane (dcpm) and 1,2-bis(dicyclohexylphosphino)ethane (dcpe) in CH_2Cl_2. After removal of solvent and washing the residue with benzene and hexane, complexes **12** and **13** were obtained as colorless solids in excellent yields (Figure 5). The observation of three signals in each ^{31}P NMR spectrum led to the formulation of **12** and **13** as four-coordinate MOLPs with three inequivalent phosphorus nuclei (Table 2). The high-field ^{31}P NMR signals of **12** (δ −21.7, −26.7) are attributable to the dcpm phosphorus nuclei, which can be seen from a ^{31}P,^{1}H-COSY NMR spectrum and the coupling constants in the ^{31}P NMR spectrum, while that at δ 39.0 can be attributed to PCy_3.

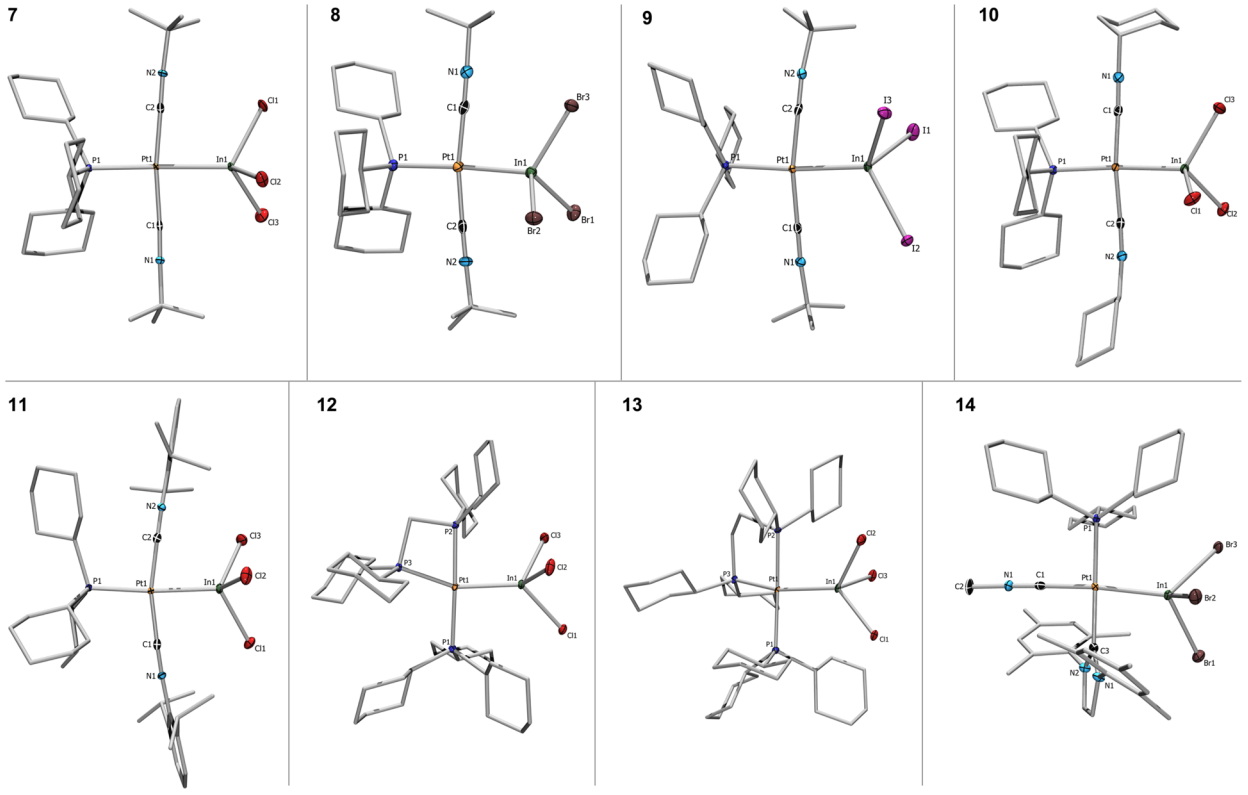

Figure 6. Crystallographically derived structures of MOLPs **2a**, **4a**, and **5a**. Thermal ellipsoids shown at the 50% probability level. Some thermal ellipsoids and all hydrogen atoms and solvent molecules (four CH_2Cl_2 in **12**, four CH_2Cl_2 in **13**, two *o*-difluorobenzene in **14**) have been removed for clarity. Selected bond lengths (Å) for **7**: Pt−In 2.6205(8). For **8**: Pt−In 2.615(2). For **9**: Pt−In 2.630(1). For **10**: Pt−In 2.6059(6). For **11**: Pt−In 2.6311(6). For **12**: Pt−In 2.6282(6), Pt−P1 2.329(1), Pt−P2 2.299(1), Pt−P3 2.351(1). For **13**: Pt−In 2.650(2), Pt−P1 2.350(7), Pt−P2 2.311(8), Pt−P3 2.327(7). For **14**: Pt−In 2.661(1).

DOI: 10.1021/jacs.6b10609
J. Am. Chem. Soc. 2016, 138, 16140−16147

Table 3. Total Electronic Energy Differences between MOLP (1a−6a) and OA Products (1b−6b)[a]

	gas	CH_2Cl_2	THF	THF (coord.)
$E_{1b}-E_{1a}$	1.74 (3.77)	5.70 (6.94)	5.41 (6.97)	−1.10 (−0.27)
$E_{2b}-E_{2a}$	0.31 (1.04)	4.32 (3.91)	4.00 (4.04)	−4.73 (−1.79)
$E_{3b}-E_{3a}$	−4.20 (−3.35)	1.70 (2.54)	1.14 (2.79)	−2.79 (−0.70)
$E_{4b}-E_{4a}$	2.91 (6.35)	9.02 (7.01)	8.53 (6.84)	−7.05 (−6.25)
$E_{5b}-E_{5a}$	3.35 (1.52)	8.90 (8.87)	8.42 (9.16)	−7.87 (−5.96)
$E_{6b}-E_{6a}$	−3.67 (−2.72)	1.88 (2.03)	4.78 (2.77)	−5.86 (−2.74)

[a]Corresponding Gibbs free energy values are in parentheses. Energies are in kcal mol^{-1}.

The low-field ^{31}P NMR signals of **13** (δ 68.4, 64.5) are clearly attributable to the dcpe phosphorus nuclei, based on the $^{31}P,^{1}H$-HMQC NMR spectrum, leading us to assign the high-field signal (δ 32.4) to PCy_3. In both **12** and **13**, the PCy_3 signal, and one of the diphosphine phosphorus nuclei (presumably that *trans* to the PCy_3), appear as doublets-of-doublets, with the remaining signal appearing as a broad singlet that does not show resolved P−P couplings or cross peaks in the $^{31}P,^{1}H$-HMQC NMR spectrum. In none of the spectra were $^{31}P-^{195}Pt$ satellites observed. The crystallographically derived structures of **12** and **13** confirmed their connectivity as square-planar MOLPs with one monophosphine and one diphosphine ligand, with the PCy_3 ligand necessarily *cis* to the $InCl_3$ unit. The most notable feature of the structures of **12** and **13** is the distorted Pt−$InCl_3$ unit, each complex having one Pt−In−Cl angle greater than 130°, in contrast to the complexes **7**−**11**, which possess Pt−In−X angles much closer to those expected for tetrahedra. Similarly, the coordination of the phosphines to the Pt center is distorted from perfect square planar due to the geometric requirements of the chelating bridges. This is most pronounced in **12**, which has a distinctly nonlinear In−Pt−P^{trans} angle (157.44(3)°).

In an attempt to extend this reactivity to the NHC-containing MOLP/OA equilibrium mixtures, mixture **5a**/**b** was treated with 3.5 equiv of the small isocyanide :CNMe. Upon cooling to −30 °C, colorless crystals precipitated (**14**; Figure 5), which provided a ^{31}P NMR signal in CD_2Cl_2 at δ 20.6, but were observed to spontaneously lose :CNMe and revert back to precursors **5a**/**b**, precluding the acquisition of reliable ^{1}H and ^{13}C NMR data. Placing the crystals under vacuum provided **5a**/**b** quantitatively. From the single crystals of **14**, a molecular structure was obtained (Figure 6) showing a Pt−In bond (2.661(1) Å, the longest observed in this study) that is slightly longer than that of **13**. This is somewhat to be expected, as **12**−**14** represent the only MOLPs in this study with four-coordinate Pt centers and two bulky ligands *cis* to the InX_3 unit. The similarity of **14** to triphosphine MOLPs **12** and **13** is also apparent from the similarly distorted Pt−$InBr_3$ unit of **14**, having one wide Pt−In−Br angle (126.29(2)°).

It should also be noted that, in general, complexes **7**−**14**, all of which contain four-coordinate Pt centers, have higher d_{rel} values than the three-coordinate MOLPs described above. This is in contrast to the analysis performed in our earlier review on MOLPs, which found that the d_{rel} value correlates very poorly with the coordination number of the donor fragment. Given also the unimposing sterics of the isocyanide ligands *cis* to the InX_3 fragment in **7**−**11**, the grounds for the dilated Pt−In bond distances must lie elsewhere, presumably in the presence of a strong donor located *trans* to the Lewis acid ligand.

DFT Calculations. Geometry minimization calculations were carried out for **1a**−**6a** and **1b**−**6b** using the ωB97XD/Def2SVP level of theory, which accurately reproduced the experimental structures. Detailed structures, frontier orbitals, and related energy levels for each complex are shown in Figures S2−S5. The HOMOs of the MOLPs **a** consist almost exclusively of Pt d_{z2} orbitals with minor contributions from the halides on the InX_3 ligand. Those of the OA products **b** consist mainly of contributions from the Pt d orbitals and orbitals on the Pt-bound halide atom, with very minor contributions from the InX_2 ligand. Upon replacing one PCy_3 ligand with IMes, there is a marked decrease in negative charge at the Pt atom, possibly caused by greater delocalization of charge across the imidazole ring of IMes. The charges of other atoms in the complexes remain relatively unchanged. In all cases, the isomerization from **a** to **b** produces an increase in the Wiberg bond index of the Pt−In bond from ca. 0.6 to ca. 0.7. This relatively small change is in line with the small contraction of the Pt−In bond observed experimentally.

The experimental observations and calculated energies of the isomers of complexes **1**−**6** revealed a clear trend: the preference for formation of MOLP **a** or oxidative addition product **b** is dependent on (1) the solvent used and (2) which halogen is involved (Cl, Br, or I). To understand these effects further, geometry optimization calculations of both isomers of compounds **1**−**6** were carried out in the solvent phase (CH_2Cl_2 and THF) using the PCM method implemented in Gaussian 09. As the PCM method is an implicit solvent method, useful to take into account bulk properties due to solvent effects, further calculations at an explicit solvent level were conducted: a set of optimizations were conducted with a molecule of THF bound directly to the In atom. The resulting energies were compared to those computed in the gas phase (Table 3).

In the gas phase, the negative energy difference calculated when X = I (**3** and **6**) indicates that the OA products **3b** and **6b** are lower in energy and therefore more stable than their corresponding MOLPs **3a** and **6a**, whereas when X = Cl, Br, the reverse is true. With solvent effects included, the same general trend is observed, with a relative decrease in preference for the formation of **a** as the halide becomes heavier. These results are in line with experimental observations.

These observations can be explained by considering that the conversion from **a** to **b** is dependent on the coordination ability of the solvent. THF is a relatively strong donor, and therefore binds to the (still-Lewis-acidic) In center, making the latter pentacoordinate. This results in the migration of one of the halides from In to Pt, and allowing the THF oxygen to bind more strongly to the more Lewis acidic In center. DCM is a poor donor and provides no electronic or steric incentive for halogen migration, resulting in less preference for the OA product **b**. The conversion from **a** to **b** is also governed by the size and electronegativity of the halogen. For the relatively small, highly electronegative Cl, **a** is favored in DCM because all three halogens can fit comfortably around In, and withdraw sufficient electron density from In to stabilize donation from Pt. When the larger, less electronegative Br is present, **a** and **b** are more equally

DOI: 10.1021/jacs.6b10609
J. Am. Chem. Soc. 2016, 138, 16140−16147

favored in DCM because of increasing steric hindrance around In and their less-effective withdrawal of electron density from In, providing an incentive for migration of Br to the Pt center. When the very large (even less electronegative) halide I is present, **b** is favored due to the greater steric crowding around In, the long In−I bonds, and poor stabilization of electron donation from Pt. It is worth noting that the polarity of the solvent also has an effect on the equilibrium between **a** and **b**, albeit only slight. A highly polar solvent will induce a degree of polarization within **a**, thus shifting the equilibrium slightly toward **b**.

In the presence of THF, the general conversion from **a** to **b** will most likely proceed via a transition state akin to that calculated for the isomerization of **3a** to **3b** (**3TS**$^{\mathbf{THF}}$, Figure 7), which

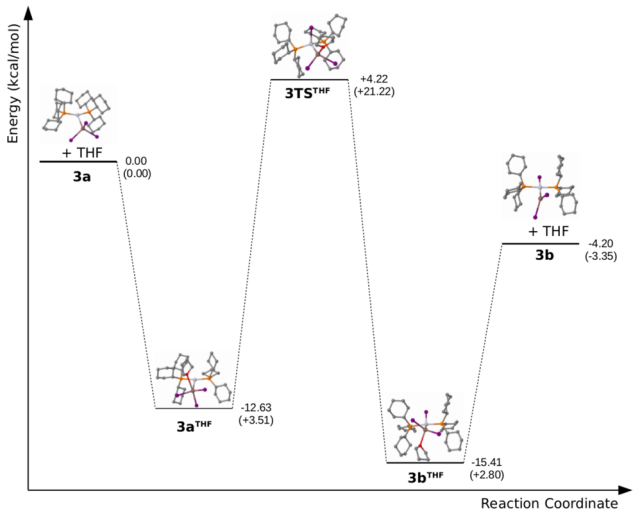

Figure 7. Calculated mechanism for the THF-mediated isomerization of **3a** to **3b**. Associated Gibbs free energy values for each species are in parentheses.

possesses an iodide bridging the In and Pt atoms ($\angle_{InPtI}$ 81.4°). The mechanism calculated for the THF-mediated isomerization of **3a** to **3b** proceeds through an intermediate with an In-bound THF molecule (**3a**$^{\mathbf{THF}}$, −12.63 kcal mol^{-1}), the transition state **3TS**$^{\mathbf{THF}}$ (+4.22 kcal mol^{-1}), and the THF adduct of **3b** (**3b**$^{\mathbf{THF}}$, −15.41 kcal mol^{-1}). Decoordination of THF finally provides **3b** and a THF molecule (−4.20 kcal mol^{-1}). This is further evidenced by the variation of entropy (reflected by the Gibbs free energy profile) (see SI) in going from the system where the THF molecule is separated to that where it is bound.

The calculations on **1a**−**6a** and **1b**−**6b**, while not intended to fully reflect the effects of the physicochemical conditions such as the actual position of equilibria, reproduce the general experimentally observed trends in the equilibria between isomers **a** and **b** well, including the effects of changing the halide and solvent. In particular, the OA-promoting effect of THF was explored in detail. The relatively small energy differences between the **a** and **b** isomers provide a rationale for the observation of equilibria in these compounds.

CONCLUSIONS

Herein, we present the observation of highly unusual equilibria in which strongly polar E−X bonds are broken and formed at a metal center. The results herein have considerable bearing on our understanding of oxidative addition processes, and suggest that MOLP complexes could act as viable pre-OA states, as either alternatives or precursors to the much more well-studied σ complexes. MOLPs are thus overlooked mechanistic possibilities that may be intermediates in certain cases where the incoming molecule bears a Lewis acidic site, for example, silanes.

ASSOCIATED CONTENT

Supporting Information

The Supporting Information is available free of charge on the ACS Publications website at DOI: 10.1021/jacs.6b10609.

X-ray crystallographic data for **1b**−**6b** (CIF)
X-ray crystallographic data for **7**−**14** (CIF)
Experimental, crystallographic, and computational procedures (PDF)

AUTHOR INFORMATION

Corresponding Author

*h.braunschweig@uni-wuerzburg.de

ORCID

Holger Braunschweig: 0000-0001-9264-1726

Notes

The authors declare no competing financial interest.

ACKNOWLEDGMENTS

We gratefully acknowledge the Deutsche Forschungsgemeinschaft (H.B.), the University of Sussex (A.V.), and the EPSRC (A.V.) for financial support of this work.

REFERENCES

(1) (a) Hartwig, J. F. *Organotransition Metal Chemistry, from Bonding to Catalysis*; University Science Books: New York, 2010. (b) Labinger, J. *Organometallics* **2015**, *34*, 4784−4795.
(2) (a) Kunin, A. J.; Johnson, C. E.; Maguire, J. A.; Jones, W. D.; Eisenberg, R. *J. Am. Chem. Soc.* **1987**, *109*, 2963−2968. (b) Deutsch, P. P.; Eisenberg, R. *Chem. Rev.* **1988**, *88*, 1147−1161.
(3) (a) Corey, J. C.; Braddock-Wilking, J. *Chem. Rev.* **1999**, *99*, 175−292. (b) Lin, Z. *Chem. Soc. Rev.* **2002**, *31*, 239−245. (c) Nikonov, G. I. *Adv. Organomet. Chem.* **2005**, *53*, 217−309. (d) Lachaize, S.; Sabo-Etienne, S. *Eur. J. Inorg. Chem.* **2006**, *2006*, 2115−2127. (e) Corey, J. Y. *Chem. Rev.* **2011**, *111*, 863−1071.
(4) (a) Lin, Z. *Struct. Bonding (Berlin)* **2008**, *130*, 123−148. (b) Alcaraz, G.; Helmstedt, U.; Clot, E.; Vendier, L.; Sabo-Etienne, S. *J. Am. Chem. Soc.* **2008**, *130*, 12878−12879. (c) Ghaffari, B. A.; Vanchura, B. A., II; Chotana, G. A.; Staples, R. J.; Holmes, D.; Maleczka, R. E., Jr.; Smith, M. R., III *Organometallics* **2015**, *34*, 4732−4740.
(5) (a) Buchanan, J. M.; Stryker, J. M.; Bergman, R. G. *J. Am. Chem. Soc.* **1986**, *108*, 1537−1550. (b) Periana, R. A.; Bergman, R. G. *J. Am. Chem. Soc.* **1986**, *108*, 7332−7346. (c) Hall, C.; Perutz, R. N. *Chem. Rev.* **1996**, *96*, 3125−3146.
(6) Levy, C. J.; Puddephatt, R. J. *J. Chem. Soc., Chem. Commun.* **1995**, 2115−2116.
(7) (a) Roy, A. H.; Hartwig, J. F. *J. Am. Chem. Soc.* **2001**, *123*, 1232−1233. (b) Roy, A. H.; Hartwig, J. F. *J. Am. Chem. Soc.* **2003**, *125*, 13944−13945.
(8) Osakada, K.; Maeda, M.; Nakamura, Y.; Yamamoto, T.; Yamamoto, A. *J. Chem. Soc., Chem. Commun.* **1986**, 442−443.
(9) Braunschweig, H.; Brenner, P.; Dewhurst, R. D.; Guethlein, F.; Jimenez-Halla, J. O. C.; Radacki, K.; Wolf, J.; Zöllner, L. *Chem. - Eur. J.* **2012**, *18*, 8605−8609.
(10) Canty, A. J.; Denney, M. C.; Patel, J.; Sun, H.; Skelton, B. W.; White, A. H. *J. Organomet. Chem.* **2004**, *689*, 672−677.
(11) Bauer, J.; Braunschweig, H.; Damme, A.; Radacki, K. *Angew. Chem., Int. Ed.* **2012**, *51*, 10030−10033.
(12) Braunschweig, H.; Brenner, P.; Dewhurst, R. D.; Krummenacher, I.; Pfaffinger, B.; Vargas, A. *Nat. Commun.* **2012**, *3*, 872.
(13) Bauer, J.; Braunschweig, H.; Dewhurst, R. D. *Chem. Rev.* **2012**, *112*, 4329−4346.

DOI: 10.1021/jacs.6b10609
J. Am. Chem. Soc. 2016, 138, 16140−16147

(14) (a) Braunschweig, H.; Gruss, K.; Radacki, K. *Angew. Chem., Int. Ed.* **2007**, *46*, 7782−7784. (b) Braunschweig, H.; Gruss, K.; Radacki, K. *Inorg. Chem.* **2008**, *47*, 8595−8597. (c) Bauer, J.; Braunschweig, H.; Dewhurst, R. D.; Radacki, K. *Chem. - Eur. J.* **2013**, *19*, 8797−8805. (d) Hupp, F.; Ma, M.; Kroll, F.; Jimenez-Halla, J. O. C.; Dewhurst, R. D.; Radacki, K.; Stasch, A.; Jones, C.; Braunschweig, H. *Chem. - Eur. J.* **2014**, *20*, 16888−16898. (e) Braunschweig, H.; Dewhurst, R. D.; Hupp, F.; Schneider, C. *Chem. Commun.* **2014**, *50*, 15685−15688. (f) Braunschweig, H.; Dewhurst, R. D.; Hupp, F.; Kaufmann, C.; Phukan, A. K.; Schneider, C.; Ye, Q. *Chem. Sci.* **2014**, *5*, 4099−4104. (g) Braunschweig, H.; Celik, M. A.; Dewhurst, R. D.; Heid, M.; Hupp, F.; Sen, S. S. *Chem. Sci.* **2015**, *6*, 425−435. (h) Braunschweig, H.; Dewhurst, R. D.; Hupp, F.; Wolf, J. *Chem. - Eur. J.* **2015**, *21*, 1860−1862. (i) Braunschweig, H.; Brunecker, C.; Dewhurst, R. D.; Schneider, C.; Wennemann, B. *Chem. - Eur. J.* **2015**, *21*, 19195−19201. (j) Braunschweig, H.; Dewhurst, R. D.; Schneider, C. *Organometallics* **2016**, *35*, 1002−1007. (k) Bissert, R.; Braunschweig, H.; Dewhurst, R. D.; Schneider, C. *Organometallics* **2016**, *25*, 2567−2573.

(15) (a) Maseras, F.; Lledós, A.; Clot, E.; Eisenstein, O. *Chem. Rev.* **2000**, *100*, 601−636. (b) Balcells, D.; Clot, E.; Eisenstein, O. *Chem. Rev.* **2010**, *110*, 749−823. (c) Zeng, G.; Sakaki, S. *Inorg. Chem.* **2011**, *50*, 5290−5297.

(16) (a) Charmant, J. P. H.; Fan, C.; Norman, N. C.; Pringle, P. G. *Dalton Trans.* **2007**, 114−123. (b) Braunschweig, H.; Brenner, P.; Mueller, A.; Radacki, K.; Rais, D.; Uttinger, K. *Chem. - Eur. J.* **2007**, *13*, 7171−7176. (c) Braunschweig, H.; Radacki, K.; Uttinger, K. *Inorg. Chem.* **2007**, *46*, 8796−8800. (d) Bauer, J.; Braunschweig, H.; Kraft, K.; Radacki, K. *Angew. Chem., Int. Ed.* **2011**, *50*, 10457−10460.

(17) Cordero, B.; Gomez, V.; Platero-Prats, A. E.; Reves, M.; Echeverria, J.; Cremades, E.; Barragan, F.; Alvarez, S. *Dalton Trans.* **2008**, 2832−2838.

DOI: 10.1021/jacs.6b10609
J. Am. Chem. Soc. 2016, 138, 16140−16147